Mathematical Geology, Vol. 32, No. 7, 2000

Derivatives of Spatial Variances of Growing Windows and the Variogram[1]

J. A. Vargas-Guzmán,[2] D. E. Myers,[3] and A. W. Warrick[4]

Geostatistical analysis of spatial random functions frequently uses sample variograms computed from increments of samples of a regionalized random variable. This paper addresses the theory of computing variograms not from increments but from spatial variances. The objective is to extract information about the point support space from the average or larger support data. The variance is understood as a parametric and second moment average feature of a population. However, it is well known that when the population is for a stationary random function, spatial variance within a region is a function of the size and geometry of the region and not a function of location. Spatial variance is conceptualized as an estimation variance between two physical regions or a region and itself. If such a spatial variance could be measured within several sizes of windows, such variances allow the computation of the sample variogram. The approach is extended to covariances between attributes that lead to the cross-variogram. The case of nonpoint sample support of the blocks or elements composing each window is also included. A numerical example illustrates the application of this conceptualization.

KEY WORDS: scales; multiresolution; moving windows; regularized variograms; spatial variances; spatial covariances.

INTRODUCTION

Estimation of a sample variogram, to characterize a point support random function $Z(x)$, may need a large number of samples on an irregular sampling grid to release information about many lag distances. The variogram $\gamma(h)$ represents the expected dissimilarity between any pair of random variables $Z(x_i)$, separated a lag distance h, where $Z(x)$ is an intrinsic stationary random function (Matheron, 1971). A sample variogram $\hat{\gamma}(h)$ is estimated from square increments computed

[1]Received 6 January 1999; accepted 18 August 1999.
[2]Department of Hydrology and Water Resources, University of Arizona, Harshbarger 250 A, Tucson, Arizona 85721.
[3]Department of Mathematics, University of Arizona, Tucson, Arizona 85721.
[4]Department of Soil, Water and Environmental Science, University of Arizona, Shantz 429 Tucson, Arizona 85721.

from a sample set of values $z(x_i)$ taken at several locations x_i. That is,

$$\hat{\gamma}(h) = \frac{1}{N(h)} \sum_{k=1}^{N(h)} (z(x_i) - z(x_i + h))^2 \tag{1}$$

where $z(x_i)$ represents a single sample of $Z(x_i)$, and $N(h)$ is the number of pairs at some lag distance h. Obviously, this approach requires a large number of pairs $N(h)$ to give a good estimate. This may be possible when a dense regular sampling grid is used. Otherwise, grouping the increments into distance classes is commonly used to enhance the number of pairs. This is done by allowing some tolerance in the vectors of lag distances. Even in the case of a regular sampling grid, grouping is frequently needed. Thus, a tolerance angle, a lag tolerance, and a bandwidth distance are selected subjectively for grouping classes (Journel and Huijbregts, 1978; Myers and others, 1982). Obviously, this subjectivity affects the uniqueness of the sample variogram. Warrick and Myers (1987) developed an optimum sampling strategy by minimizing the square differences between a desired and obtained frequency distribution for lag distances grouped into classes. They found that such an optimum sampling strategy for computing variograms at small lag distances is obtained from a nonregular grid.

To solve the problem of computing variograms from an irregular sampling grid, Sen (1989) proposed avoiding the grouping algorithm by using a cumulative variogram:

$$\gamma_C(u) = \int_0^u \gamma(h)\, dh \tag{2}$$

The integral of the variogram is related to the auxiliary function χ, which has been used by earlier authors of geostatistics for computing the average variogram of a fixed point and a line segment A-B (Clark, 1976; Journel and Huijbregts, 1978):

$$\chi = \frac{1}{\upsilon} \int_A^B \gamma(u)\, du \tag{3}$$

where υ is the size of the segment A-B. However, Myers (1994) pointed out that the numerical integration of Equation (2) proposed by Sen (1989) was not accounting for the irregular spacing of the data. Later on, Delay and de Marsily (1994) proposed a numerical integration to account for such an irregular spacing of the data. In such a way, they suggested the integral of the variogram can be used to adjust the variogram. The paradigm of computing the sample variogram from increments was maintained because they are needed to obtain the numerical integral of the variogram.

A related problem, as soon will be apparent, is to compute point support variograms when the studied attribute is too tiny to be sampled at point support or the measuring sampling devise is too large to attempt collecting samples at smaller support. Examples of this problem may be the size of grains of soil and features of individual microbes which can not be measured individually. Other examples are ground features such as vegetation that can not be captured in detail from a satellite. In such cases, scientists average the attribute within a sample τ of volume υ and express the attribute as an average feature (e.g., percentage of sand content). That is,

$$Z_{\upsilon}(y_j) = \frac{1}{\upsilon} \int_{\tau} Z(x_i)\, dx \tag{4}$$

where $Z_{\upsilon}(y_j)$ may be interpreted as an average random variable at location y_j or a nonpoint support random variable. Notice that y_i is the spatial location of the center of the region τ. A regularized random function may be introduced $Z_{\upsilon}(y)$ and its variogram computed for such spatial support υ is called regularized variogram. However, we may need to know the point support variogram. In the case of remote sensing, increasing resolution is a non trivial problem. Sampling at point support, in the examples mentioned above may be problematic, so a new approach that allows to estimate the point support variogram from the average or larger support is needed.

The averaging approach of Equation (4) affects the variance between the elements and is quantitatively explained (Journel and Huijbregts, 1978). The average variogram function computed from point support locations is

$$\bar{\gamma}(\upsilon, \upsilon') = \frac{1}{\upsilon\upsilon'} \int_{\tau} dx \int_{\tau'} \gamma(x - x')\, dx' \tag{5}$$

where υ and υ' are the size of two regions, τ and τ'. Note that Equation (5) allows the regions to be separated but for our purposes they overlap and coincide forming a single sample or region element τ. In two dimensions, for example, all the elements τ are like disjoint rectangles making a mosaic within a larger rectangular region φ of size V. Then, Equation (5) may be applied for the average variogram within the larger region φ. This leads to

$$\bar{\gamma}(V, V') = \frac{1}{VV'} \int_{\varphi} dx \int_{\varphi'} \gamma(x - x')\, dx' \tag{6}$$

where, for our purposes, φ and φ' overlap forming a single window composed of disjoint elements τ. From the early works of geostatistics developed by Krige and Matheron, it is known that the dispersion variance $D^2(\upsilon \mid V)$ is the spatial variance between the spatial elements τ within the domain φ (Journel and Huijbregts, 1978).

That is,

$$D^2(\upsilon \mid V) = \bar{\gamma}(V, V) - \bar{\gamma}(\upsilon, \upsilon) \tag{7}$$

For elements of point support ($\upsilon \to 0$) this is

$$D^2(0 \mid V) = \bar{\gamma}(V, V) \tag{8}$$

A generic name for the average variogram and dispersion variances within a spatial window is *spatial variance*.

In this paper, we show that it is possible to go back from spatial variances, such as Equation (7), to the point support variogram. This approach is not a practical alternative to Equations (1) or (2), but it may be useful for examples like those mentioned above. The proposed approach introduces a new paradigm, which is to measure spatial variances within windows and use them for computing a variogram. This assumes that we could take an individual sample of support V (e.g., soil sample) and measure an average attribute and its included spatial variance. This could be done in some cases with an analytical instrument scanning space and measuring the attribute and its spatial variance within windows for larger and larger physical sizes V. The process might be repeated for several locations and "samples" that systematically overlap in moving and growing windows. Then, as we show later, we can use the spatial variances, as a function of the size of the window, to estimate the variogram. This paper develops the theory and includes a practical example of computing variograms from data of spatial variances by analysis of the effect of growing windows on spatial variances.

THEORY OF DERIVATIVES OF SPATIAL VARIANCES

Physical Size and Spatial Variances

The variogram for an intrinsic random function $Z(x)$ is defined as

$$\gamma_z(h) = \frac{1}{2}E(Z(x_i) - Z(x_i + h))^2 \tag{9}$$

A second random function $Y(x)$ proportional to $Z(x)$ may be introduced as follows:

$$Y(x) = CZ(x) \tag{10}$$

where C is an arbitrary constant. Then,

$$\gamma_Y(h) = \frac{1}{2}E(CZ(x_i) - CZ(x_i + h))^2 \tag{11}$$

This leads to

$$\gamma_Y(h) = C^2 \gamma_Z(h) \tag{12}$$

Applying Equations (6) and (12), the average variogram function within a block φ for the random function $Y(x)$ is

$$\bar{\gamma}_Y(V, V') = \frac{1}{VV'} \int_{\varphi} dx \int_{\varphi'} C^2 \gamma_Z(x - x')\, dx' \tag{13}$$

This yields

$$\bar{\gamma}_Y(V, V') = C^2 \gamma_Z(V, V') \tag{14}$$

Notice in Equation (13) that V represents the size or a constant number, and for a single physical region or window $V = V'$, we can chose C such that

$$C = V \tag{15}$$

From Equation (13) this leads to

$$\bar{\gamma}_Y(V, V') = \int_{\varphi} dx \int_{\varphi'} \gamma_Z(x - x')\, dx' \tag{16}$$

Equations (14)–(16) imply that $Y(x)$ is a random function that has an average variogram function equal to the *total* spatial variance of the random function $Z(x)$ within a window φ of size V. As soon will be apparent, this analysis also applies to higher dimensions.

Analogously to Equation (7), the dispersion variance $G^2(\upsilon \mid V)$ for $Y(x)$ is

$$G^2(\upsilon \mid V) = \bar{\gamma}_Y(V, V) - \bar{\gamma}_Y(\upsilon, \upsilon) \tag{17}$$

Applying Equation (14) for both average variogram functions in Equation (17) yields

$$G^2(\upsilon \mid V) = C^2 \bar{\gamma}_Z(V, V) - C^2 \bar{\gamma}_Z(\upsilon, \upsilon) \tag{18}$$

and using Equation (15) this is

$$G^2(\upsilon \mid V) = V^2 D^2(\upsilon \mid V) \tag{19}$$

where $D^2(\upsilon \mid V)$ is the dispersion variance of $Z(x)$ as Equation (7). Notice that $Y(x)$ is different for each value of V chosen.

The support of a region φ^t includes size V and shape and can be measured as a length for $t = 1$, an area for $t = 2$ or a volume for $t = 3$. Individual points can be represented in rectangular, polar, cylindrical, spherical, or even curvilinear location coordinates $x_1 \ldots x_d$. The isotropic variogram $\gamma_Z(h)$ as classically defined is a function of the separation distance h, which can be expressed in any system of location coordinates. Moreover, the size of a window (block or pixel) V can be measured by a set of variables $w_1 \ldots w_d$ that are parallel to $x_1 \ldots x_d$. For example, for a rectangular window the variables $\{w_1, w_2\}$ are the sides along the two perpendicular sides and the area of the block is given by a product $V = w_1 w_2$. V represents volume, area, or length or any dimensional support. Variables $w_1 \ldots w_d$ are just features like sides or radius of the window, and implicitly describe its shape too.

In the classical computation of average variograms and dispersion variances, the support of the region is constant. Now we introduce a new approach in which the size of the window V is a variable or a set of variables. We call this approach growing windows. For a straight line segment $V = w$. However, we hold the support constant for the elements υ within the window. That is, $\bar{\gamma}_Z(\upsilon, \upsilon) = k$ is also a constant. Then,

$$G^2(w) = \bar{\gamma}_Y(w, w) - \bar{\gamma}_Y(\upsilon, \upsilon) \tag{20}$$

Because $Y(x) = wZ(X)$, now $Y(x)$ is different for each size of window. Notice that for a single window, w is a constant value. The last equation can be written in a more explicit form as

$$G^2(w) = \int_0^w dx \int_0^w \gamma_Z(x - x')\, dx' - w^2 k \tag{21}$$

This $G^2(w)$ function allows computation of the point support variogram whether k is also known. Recall from Equation (7) that the dispersion covariance $D^2(\upsilon \mid V)$, for constant υ and variable $V = w$, in one dimension can be written as $D^2(w) = D^2(\upsilon \mid V)$, where we avoid using the symbol of the constant υ for simplicity. Then,

$$G^2(w) = w^2 D^2(w) \tag{22}$$

In higher dimensions, the window can grow even when a single variable w_1 is increasing and other variables $w_2 \ldots w_d$ are held constant. A constant window shape is also required. For example, rectangles with sides parallel to the axes, whatever their sizes, are considered the same shape.

Derivative of a Spatial Variance Function

Assuming point support for the elements τ within any window, the $G^2(w)$ function defined in Equation (21) becomes

$$G^2(w) = \int_0^w dx \int_0^w \gamma_Z(x - x')\, dx' \tag{23}$$

By applying the Cauchy–Gauss method, this equation can be rewritten as

$$G^2(w) = 2\int_0^w \left(\int_0^w \gamma(h)\, dh\right) dh \tag{24}$$

From this it is evident that

$$\gamma(h) = \frac{\partial^2(G^2(w))}{2\partial w^2} \tag{25}$$

where $h = w$ in one dimension. Substituting Equation (22) into (25) results in

$$\gamma(h) = \frac{\partial^2(w^2 D^2(w))}{2\partial w^2} \tag{26}$$

This last equation provides the algorithm for computing variograms from spatial variances. In Cartesian coordinates, two-dimensional windows need four derivatives and three dimensional windows need six derivatives. For a parallelepiped, the $G^2(w_1 w_2 w_3)$ function is

$$G^2(w_1 w_2 w_3) = w_1^2 w_2^2 w_3^2 D^2(w_1 w_2 w_3) \tag{27}$$

This is the same as for Equation (19) because $V = w_1 w_2 w_3$ is the volume of the window.

The derivative of the total variance function $G^2(w)$ with respect to w is the rate of change of the total variance due to change of the size of the window along w. For several variables w_i, the classical definition of derivative is given by

$$\left[\frac{\partial G^2(w_1 \ldots w_d)}{\partial w_i}\right]_{w_{j \neq i}} = \lim_{\Delta w_i \to 0} \frac{(G^2(w_i + \Delta w)|w_{j\neq i}) - (G^2(w_i) \mid w_{j\neq i})}{\Delta w_i} \tag{28}$$

To interpret this equation, see Figure 1. The window is composed of two regions both centered and coinciding in the same physical space; the first is φ^t of support V and the second is φ^s of support V', where $V = V'$. The differential of size dw in

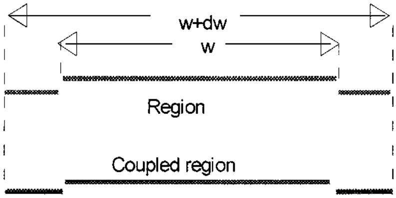

Figure 1. A centered region and its couple growing at both extremes. The growing segments are differentials.

one dimension means a change of the support of the window and implies two new extreme zones are annexed to both (coinciding) regions. For higher dimensions this is ∂w. For a region that grows on two opposite directions, we can easily interpret that any change in size ∂w produces a $\partial(G^2(w))$ that is the total variance between $2\partial\varphi^s$ (the extremes in one region) and the coupled region $\varphi^t + 2\partial\varphi^s$ in the w direction. Therefore, a single derivative of $G^2(w)$ with respect to w is twice the variance between the window of topologic dimension t of size w and a lower topology region $s = t - 1$ and size ∂w. A second derivative can be taken with respect to the same coordinate. In such a case, the topology of the region and the coupled region are equated again $s - 1 = t - 1$. Consider several size variables $(w_1 \ldots w_d)$; then Equation (26) becomes more complicated and can be written as

$$\gamma(h) = \frac{\partial^2}{2F\partial(w_d)^2}\left[w_d^2\left[\cdots\left(\lim_{w_i\to 0}\left[\frac{\partial^2 w_i^2[D^2(w_1\ldots w_d)]}{\partial^2 w_i}\right]\right)\right]\right] \tag{29}$$

where d is total number of variables measuring the size of the window, F is the number of coordinates allowing growth on two opposite directions, and h is an Euclidean separation distance function

$$h = f(w_1 \ldots w_d) \tag{30}$$

The computation of the limit in Equation (29) is needed to get variances that are for overlapped and coincident regions. This will become clear after the case of rectangular windows is analyzed.

The Derivative of Variances of a Growing Straight Segment

A straight line segment A-B is defined in a Cartesian system and the variance within the segment changes by changing the length of A-B. The support of a segment A-B of the line is given by the value w. The function $G^2(w)$ for the random function $Z(x)$ is given by Equation (21). From the above concepts, the line A-B grows in opposite directions along w. A ∂w differential of w implies two points A' and B' are added to the extremes. The variances added are between a point and a segment Var(A', A'-B') and Var(B', A'-B'). Then, by symmetry the variance added is twice a point-segment variance as predicted by the theory. This is

$$\frac{\partial(G^2(w))}{\partial w} = 2w\chi \tag{31}$$

where χ is the auxiliary function of Equation (3). Note that the line *A-B* has a topological dimension $t = s = 1$. However, the differential ∂w has $s = 0$. A point-line average variance χ has $t = 1$ and $s = 0$. So one more derivative with respect to w (for the coupled region) is required to achieve $t = s = 0$ and the variogram $\gamma(h)$, where $h = w$, and

$$\frac{\partial(w\chi)}{\partial w} = \gamma(h) \tag{32}$$

This two-step approach is equivalent to Equation (25). From the formulas it is easy to see that the integral of the variogram is the total variance of two regions where the topological dimensions are $t = 1$ and $s = 0$, respectively. For a segment of length w, this is

$$w\chi = \int_A^B \gamma(h)\,dh \tag{33}$$

The integral of the variogram is the total variance between a point A and a line A-B. In a continuous sense, from Equation (31), $w\chi$ is half the rate of change of the total variance in a segment when the domain grows. Therefore, the cumulative variogram (Sen, 1989), the integral of the variogram (Delay and de Marsily, 1994), and the auxiliary function χ multiplied by w described in Journel and Huijbregts (1978) are mathematically the same and can be obtained from derivatives of higher dimensional spatial variances.

The Derivative of Variances in a Growing Rectangle

Spatial variances within rectangular windows increase as the size or support of the window increases and this fact may be used for computing variograms. Rectangular blocks fit exactly into a rectangular field, and blocks are commonly used in mining and agriculture. For this reason, rectangles have been extensively used for estimation purposes such as block kriging. There is considerable pertaining computation of dispersion variances from univariate variograms for rectangular regions (Clark, 1976; Journel and Huijbregts, 1978; Rendu, 1978). Applying our approach, growing rectangular blocks may be used for computation of variograms when variances inside those blocks are known.

For applying the derivative of variances theory to a growing rectangle, the variance data should come from rectangles or windows measured at different sizes. The simplest way to describe the points in a rectangular region and its coupled region is with a Cartesian system. Under isotropic conditions, the rectangles could be rotated at different angles and the data still would be applicable. However, under anisotropic conditions the windows should preserve the orientation because directional derivatives might generate directional variograms.

The variance inside a rectangular block $D^2(p, q)$ is given as the average value conditioned to the size of the region measured by its sides p and q. The total variance $G^2(p, q)$, function of the Cartesian coordinates (p, q), following Equation (19), is

$$G^2(p, q) = p^2 q^2 D^2(p, q) \tag{34}$$

Function $D^2(p, q)$ describes the average spatial variance as the sides of the window p and q changes. The first derivative of $G^2(p, q)$ with respect to p gives twice the total variance between the border line along q and the rectangle. So the second derivative with respect to p gives a line–line variance in the direction of q. The limit when p goes to zero gives the variance of a segment of a line along q coinciding with itself. Then, two derivatives with respect to q give twice the directional variogram in the direction of q. For other directional variograms, rotated rectangles should be considered. For the variogram in the direction of the coordinate q, Equation (29) is expressed as

$$\gamma(h) = \frac{\partial^2}{2\partial q^2}\left(q^2\left(\lim_{p\to 0}\left[\frac{\partial^2[p^2 D^2(p, q)]}{2\partial p^2}\right]\right)\right) \tag{35}$$

where the lag distance h for any two points into the rectangular window is given by

$$h = \sqrt{p^2 + q^2} \tag{36}$$

The Derivative of Spatial Covariances Between Attributes

The dispersion (cross) covariance $D^2_{Z_1 Z_2}(w_1 \ldots w_d)$ between two random functions $Z_1(x)$ and $Z_2(x)$ (e.g., geological features) is an extension of Equation (7) to multivariate geostatistics (Vargas-Guzmán, Warrick, and Myers, 1999). Such within-window covariance is expected to change as the size of the window grows. The average cross-variogram function needed to define dispersion (cross) covariances $D^2_{Z_1Z_2}(w_1 \ldots w_d)$ is

$$\bar{\gamma}(V, V') = \frac{1}{VV'} \int_{\varphi} dx \int_{\varphi'} \gamma_{Z_1Z_2}(x - x')\, dx' \tag{37}$$

where $\gamma_{Z_1Z_2}(h)$ is the cross-variogram. Extending Equation (29) to this case gives the possibility of computing the cross-variogram from covariances. That is,

$$\gamma_{Z_1Z_2}(h) = \frac{\partial^2}{2F\,\partial(w_d)^2}\left[w_d^2\left[\cdots\left(\lim_{w_i\to 0}\left[\frac{\partial^2 w_i^2[D^2_{z_1z_2}(w_1 \ldots w_d)]}{\partial^2 w_i}\right]\right)\right]\right] \tag{38}$$

where h is again the distance that is a function of the location coordinates. For example, in one dimension the cross-variogram is obtained with half of two derivatives of the total dispersion (cross)-covariance between attributes.

The Derivative of Variances for Nonpoint Support

For many purposes of land management, mining, environmental contamination clean up, remote sensing, and other applications, the domain is divided in blocks or nonpoint elements. Commonly elements τ of size υ are taken in such a way that they make up exactly the window φ of size V. We want to analyze what happens to the $G^2(w)$ function and its derivatives when one dimensional elements of constant size υ have nonpoint support.

From Krige's formula, it is well known that the expected point variance in a window φ is the sum of the expected point variance *within* the elements τ and the dispersion variance *between* elements τ; this is implicit in Equation (7). Then, assuming a constant element size υ and windows of variable size w, a total variance function following Equation (17) is

$$G^2(w) = w^2\bar{\gamma}(w, w) - w^2\bar{\gamma}(\upsilon, \upsilon) \tag{39}$$

where w is the size of φ, and υ is the size of elements τ along the same direction as w. The simplest case would be when the size υ of the element is held constant; then

$$\bar{\gamma}(\upsilon, \upsilon) = k \tag{40}$$

and

$$G^2(w) = w^2 D^2_{(\upsilon|w)}(w) = w^2\bar{\gamma}(w, w) - kw^2 \tag{41}$$

Thus, it follows that

$$\frac{\partial^2[w^2 D^2_{(\upsilon|w)}(w)]}{2F\partial(w)^2} = \gamma(h) - k \tag{42}$$

Therefore, Equation (25) applied to this case gives the regularized variogram for $h \geq \upsilon$

$$\gamma_\upsilon(h) = \gamma(h) - k \tag{43}$$

Application to Finite Growth

The derivative of variance can be applied to the analysis of the change of variance when the region φ^t of size u grows becoming a region ϑ^t of size υ. In this case, we wish to find the average variogram function $\overline{\gamma}(u, \upsilon)$ between the centered regions φ^t and ϑ^t from the elementary average variogram functions $\overline{\gamma}(u, u)$ and $\overline{\gamma}(\upsilon, \upsilon)$. Consider a straight segment of size u; then the segment grows on both directions to a size υ. The growth is $2m$, where $2m = \upsilon - u$. From the derivative of the variance explained before, the change of variance is

$$\upsilon^2\overline{\gamma}(\upsilon, \upsilon) - u^2\overline{\gamma}(u, u) = 2[m^2\overline{\gamma}(m, m) + mu\overline{\gamma}(m, u)] \tag{44}$$

where $\overline{\gamma}(m, m)$ is the variance within the growth at one extremity of size m and $\overline{\gamma}(m, u)$ is the variance between the growth at one extremity and the initial region of size u. It follows that

$$\upsilon^2\overline{\gamma}(\upsilon, \upsilon) - 2m^2\overline{\gamma}(m, m) = 2mu\overline{\gamma}(m, u) + u^2\overline{\gamma}(u, u) = u\upsilon\overline{\gamma}(u, \upsilon) \tag{45}$$

and

$$\overline{\gamma}(u, \upsilon) = \frac{\upsilon^2\overline{\gamma}(\upsilon, \upsilon) - 2\left[\left(\frac{u-\upsilon}{2}\right)^2\overline{\gamma}\left(\frac{u-\upsilon}{2}, \frac{u-\upsilon}{2}\right)\right]}{u\upsilon} \tag{46}$$

This equation can be useful for finding analytical expressions $\overline{\gamma}(u, \upsilon)$ for blocks ϑ^t and φ^t when $\overline{\gamma}(\upsilon, \upsilon)$ and $\overline{\gamma}(m, m)$ are known. The limitation is that this equation assumes ϑ^t is centered with respect to φ^t. When φ^t and ϑ^t are not centered, or if they are displaced a distance h, the analysis with the result should be different. A change of the distances between blocks can change the average variogram $\overline{\gamma}(u, \upsilon)$. Therefore, relative locations of φ^t and ϑ^t can affect the variance between different blocks. This is related to the case of a cross-support variogram (i.e., a cross-variogram where two supports u, v are treated as two attributes), which is not considered here.

PRACTICAL APPLICATIONS

Variograms from Numerical Variances

An exhaustive simulated realization of a regionalized random variable has been obtained by simulated annealing with GSLIB (Deutsch and Journel, 1992). The distribution of the simulated realization is normal. The numerical variogram of the realization is the same as the theoretical model used in the simulation which is nested with a nugget 0.2 and a spherical component of range 1 m and sill 0.8. Then, $\gamma(h) = 0.2(1 - \delta(h)) + 0.8(\mathrm{sph}(1))$, where in the nugget term $\delta(h) = 1$ if $h = 0$ and $\delta(h) = 0$ otherwise, and sph(1) is the spherical component of range 1 m. The whole domain simulates a 50 m trench made by 5000 elements (Fig. 2).

Variance within a window placed on the trench is given by Equation (8). Because each one of the simulated elements is uniform, the data set represents the entire trench and Equation (6) is

$$\begin{aligned}\bar{\gamma}(V, V') &= \frac{1}{VV'} \int_V dx \int_{V'} \gamma(x - x')\, dx' \\ &= \frac{1}{n^2}\left[(n-1)\sum_1^n (z_i - \bar{z})^2 - 2\sum_{i=2}^{n}\sum_{j=1}^{i-1}(z_i - \bar{z})(z_j - \bar{z})\right] \qquad (47)\end{aligned}$$

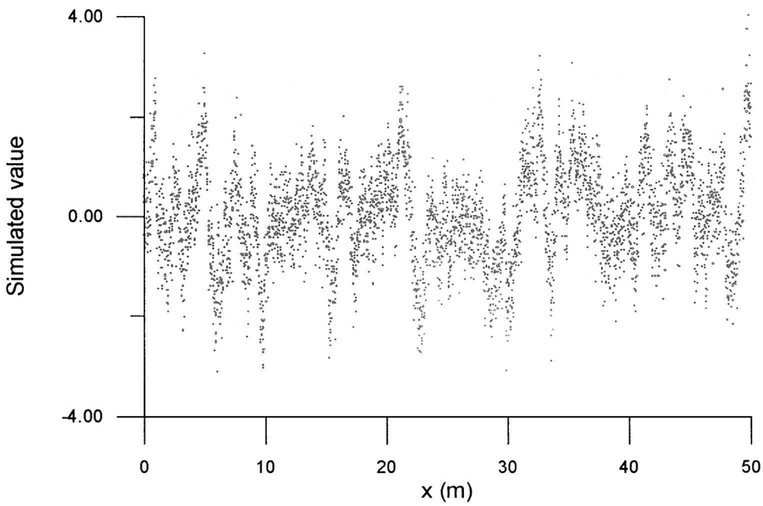

Figure 2. Simulated data set (5000) points along a 50 m trench.

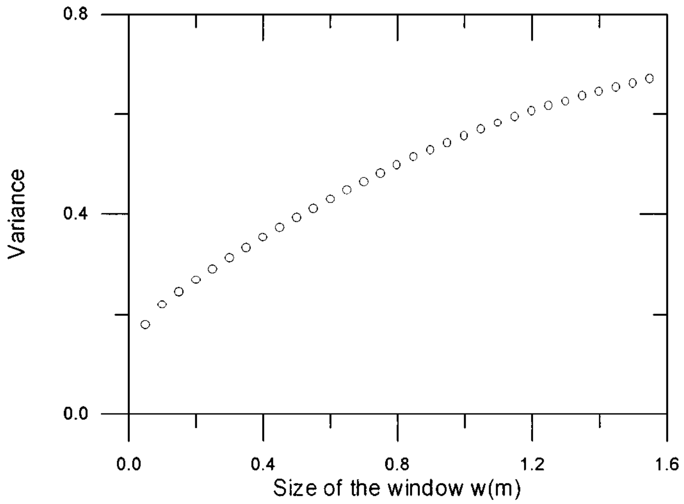

Figure 3. Variances from first sampling experiment.

where $V = n$ and $\gamma(x - x') = (z_i - z_j)^2 = (z_i - \overline{z})^2 - 2(z_i - \overline{z})(z_j - \overline{z}) + (z_j - \overline{z})^2$. Thus, for an complete data set,

$$\bar{\gamma}(V, V') = \frac{\sum_1^n (z_i - \overline{z})^2}{n} \tag{48}$$

In a first sampling experiment, windows were selected with sizes $w = \{5, 10, \ldots, 155\,\text{cm}\}$. Each size of window scanned the trench at steps of 3 cm allowing overlapping of the sequential windows. The process is like moving averages but we are interested just in the spatial variance as Equation (19). Then, for a given size of window, variances are averaged for an estimate of spatial variance $\hat{D}^2(w_i)$. The process is repeated and results are plotted in Figure 3. Then, a numerical representation of $\hat{G}^2(w) = w^2\hat{D}^2(w)$ is plotted in Figure 4. The second-order half-derivatives are computed numerically from the $\hat{G}^2(w)$ data by finite differences. The estimated sample variogram in Figure 5 resembles the corresponding model variogram Figure 7. Note the quality of the variogram is better for smaller lag distances.

The second sampling experiment takes a smaller amount of replicated sample variances by disallowing overlapping the equal size windows. So small windows have larger possibility of more replicates than larger windows. However, we increase the number of sizes of windows to be used to almost 160. The sample variances (averaged for each size of window) are displayed in Figure 6. These variances can be modeled with the equations shown in Table 1. However, we attempt to get the numerical or sample variogram. The problem is that derivatives of noisy data have exaggerated noise because of the product in $\hat{G}^2(w) = w^2\hat{D}^2(w)$.

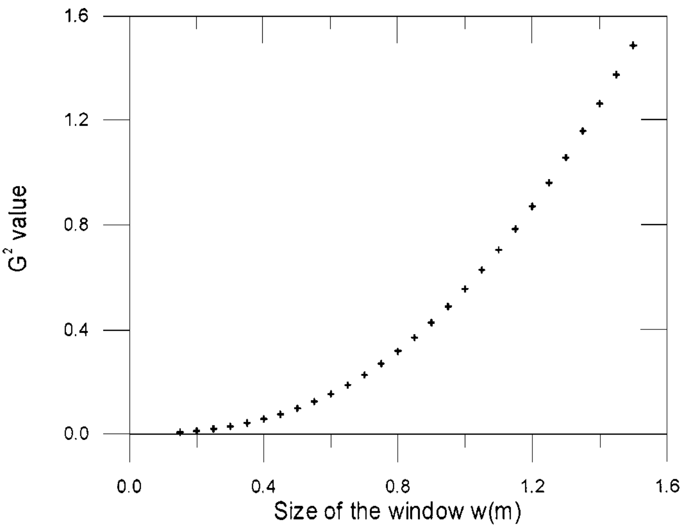

Figure 4. $G^2(w)$ estimated from first sampling experiment.

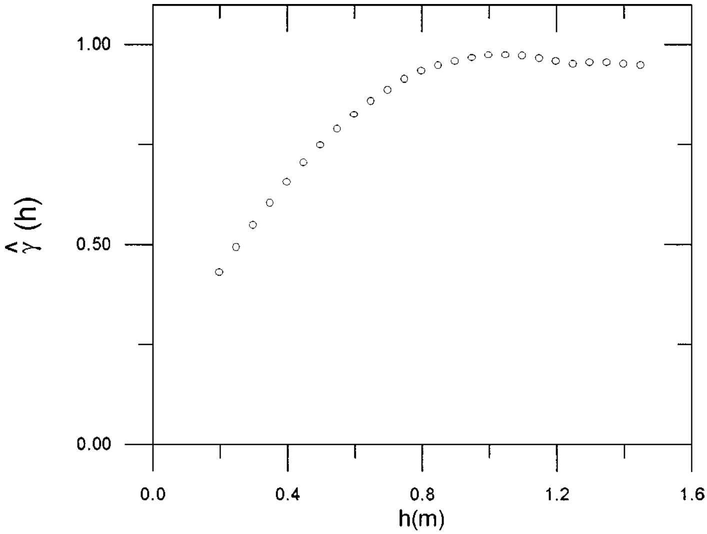

Figure 5. Sample variogram from variances of first experiment.

The variance function was smoothed by applying classic moving averages. Finite differences are used to obtain the sample variogram from $\hat{G}^2(w)$. The sample variogram and its model are shown in Figure 7. In practice, it would be advisable to model both the sample variances and the sample variogram simultaneously. Finally, we observe that it is preferable to sample only few sizes of windows but

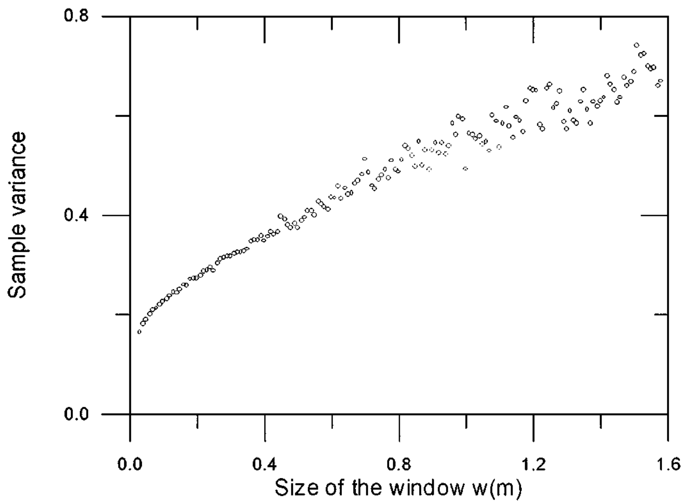

Figure 6. Variances from second sampling experiment.

with a lot of replicates of the same size of window rather than many sizes of windows with few replicates.

Application to Models of Variances

Analytical expressions for the average variograms in fixed regions provided in the literature are spatial variance functions for point support. The spatial variances for a straight segment L and a rectangular region of size V are given by Clark (1976), Journel and Huijbregts (1978), Rendu (1978), and Webster and Burgess (1984). Such relationships are expressed as auxiliary functions. In our case, we generalize them as functions of the coordinates describing the size or boundary of the growing window. $G^2(w)$ functions are computed by applying Equation (22). Then, the required operations are performed to illustrate the analytic models of variances at lower dimension.

The purpose of these examples is to compute variograms and show that the differentiation of variances is the inverse of computing auxiliary functions. However, from the conceptual point of view, derivatives of $G^2(w)$ functions are the rate of the change of variance as the window grows. On the other hand, computing auxiliary functions is an averaging concept in a single fixed size domain. For the analytical expressions analyzed below, the sill is taken constant so that it does not affect the derivatives.

Table 1 shows the models of variance and their half derivatives for straight segment windows, where $F(l)$ are models provided in the cited literature, $G^2(w)$

Table 1. Variance Models and Its Derivatives for a Straight Line

	$F(l)$	$G^2(w)$	$\frac{1}{2}\frac{\partial[G^2(w)]}{\partial w}$	$\frac{1}{2}\frac{\partial^2[G^2(w)]}{\partial w^2}$
Spherical	$\frac{1}{2}\frac{l}{a} - \frac{1}{20}\frac{l^3}{a^3} \quad \text{if } l \in (0, a)$	$\frac{1}{2}\frac{w^3}{a} - \frac{1}{20}\frac{w^5}{a^3} \quad 0 \le w \le a$	$\frac{3}{4}\frac{w^2}{a} - \frac{1}{8}\frac{w^4}{a^3} \quad 0 \le x \le a$	$\gamma(h) = \frac{3}{2}\frac{h}{a} - \frac{1}{2}\frac{h^3}{a^3} \quad 0 \le h \le a$
	$1 - \frac{3}{4}\frac{a}{l} + \frac{1}{5}\frac{a^2}{l^2} \quad \text{if } l \ge a$	$w^2 - \frac{3}{4}aw + \frac{1}{5}a^2 \quad w > a$	$w - \frac{3}{8}a \quad x > a$	$= 1 \quad h > a$
Linear	$\frac{l}{3}$	$\frac{w^3}{3}$	$\frac{w^2}{2}$	$\gamma(h) = h$
Logarithmic	$\log(l) - \frac{3}{2}$	$\frac{w^2 \log(w)}{2} - \frac{3}{4}w^2$	$w \log(w) + \frac{w}{2} - \frac{3}{2}w$	$\gamma(h) = \log(h)$
Exponential	$1 - \frac{2a}{l}\Big(1 - \frac{a}{l}(1 - e^{-(l/a)})\Big)$	$w^2 - 2aw\Big(1 - \frac{a}{x}(1 - e^{-(w/a)})\Big)$	$w^2 - 2aw\Big(1 - \frac{a}{w}(1 - e^{-(w/a)})\Big)$	$\gamma(h) = 1 - e^{-(h/a)}$
Power	$\frac{2l^\theta}{(\theta+1)(\theta+2)}$	$\frac{2w^{\theta+2}}{(\theta+1)(\theta+2)}$	$\frac{w^{\theta+1}}{\theta+1}$	$\gamma(h) = h^\theta$
Gaussian	$1 + \frac{a^2}{l^2} - \frac{a^2 \exp(-(l^2/a^2))}{l^2}$	$w^2 + a^2 - a^2 \exp\Big(-\frac{w^2}{a^2}\Big)$	$w - \frac{1}{2}a\sqrt{\pi}\ \mathrm{erf}\Big(\frac{w}{a}\Big)$	$\gamma(h) = 1 - \exp\Big(-\frac{h^2}{a^2}\Big)$
	$- \frac{a\sqrt{\pi}\ \mathrm{erf}(l/a)}{l}$	$- aw\sqrt{\pi}\ \mathrm{erf}(w/a)$		

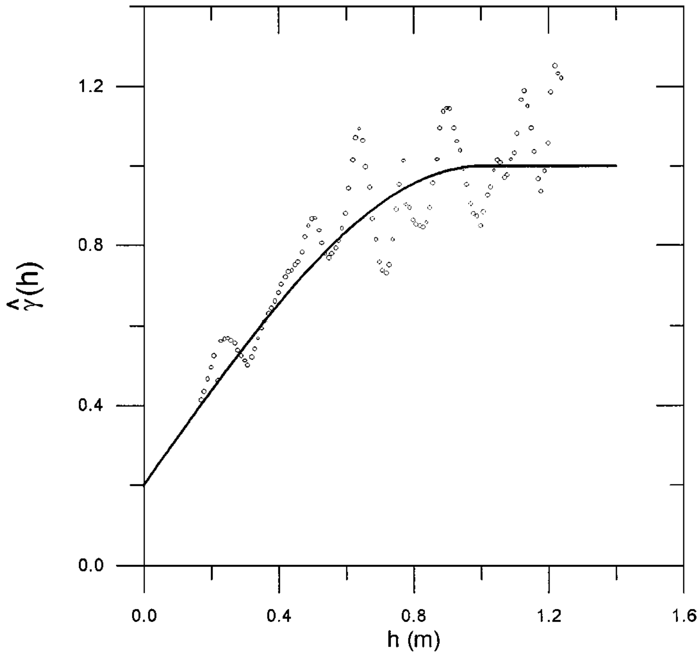

Figure 7. Model and sample variograms from variances of second experiment.

are the total directional variances, $0.5G'(w)$ and $0.5G''(w)$ are the half of the first and second derivatives respectively. Note the model variograms are easily computed in these cases. Table 1 describes domains of topological dimension of $t = 1$ that have been found most suitable for computing variograms from spatial variances. Table 2 illustrates cases for rectangular windows, and they are much more complicated models of spatial variances $F(x, q)$. Such functions are similar to the models found in Webster and Burgess (1984). Table 2 shows the analytical derivatives of $G^2(w) = q^2F^2(x, q)$. The examples follow the procedure explained before for derivative of variances in a growing rectangle. In both cases, the first two derivatives with respect to the coordinates provide a line–line variance function. Then, the computation of the limit is required to achieve a one dimensional spatial variance that is treated as described in Table 1.

Why Use Variances to Compute the Variogram?

We mention some examples in which the theory developed in this paper may be applied. In practical cases, measuring each individual “point” in the domain is impossible, so we resort to larger support random functions. This is analogous to

Table 2. Variogram from Variances in 2D Rectangles

Linear model

$$F(x,q)=\frac{q^3}{15x^2}+\frac{(x^2)^{\frac{3}{2}}}{15q^2}+\frac{1}{5}\sqrt{q^2+x^2}-\frac{q^2\sqrt{q^2+x^2}}{15x^2}-\frac{x^2\sqrt{q^2+x^2}}{15q^2}-\frac{q^2\log(q)}{6x}-\frac{x^2\log(x^2)}{12q}+\frac{x^2\log(q+\sqrt{q^2+x^2})}{6q}+\frac{q^2\log(x+\sqrt{q^2+x^2})}{6x}$$

$$\frac{\partial[G^2(x,q)]}{2\partial q}=\frac{q^4}{6x^2}+\frac{1}{4}q\sqrt{q^2+x^2}-\frac{q^3\sqrt{q^2+x^2}}{6x^2}-\frac{q^3\log(q)}{3x}-\frac{1}{24}x^2\log(x^2)+\frac{1}{12}x^2\log\left(q+\sqrt{q^2+x^2}\right)+\frac{q^3\log(x+\sqrt{q^2+x^2})}{3x}$$

$$\frac{\partial[G^2(x,q)]}{2\partial q}=\frac{2\left(q^2\right)^{\frac{3}{2}}}{3x^2}+\frac{1}{3}\sqrt{q^2+x^2}-\frac{2q^2\sqrt{q^2+x^2}}{3x^2}-\frac{q^2\log(q^2)}{2x}+\frac{q^2\log(x+\sqrt{q^2+x^2})}{x}\quad\text{and}\quad\lim_{q\to 0}\frac{\partial[G^2(x,q)]}{2\partial q}=\frac{x}{3}$$

Spherical model (q and x > range)

$$F(x,q)=\frac{q^3}{10x^2}-\frac{q^5}{105x^2}-\frac{x^4\sqrt{x^2}}{105q^2}+\frac{(x^2)^{\frac{3}{2}}}{10q^2}+\frac{3}{10}\sqrt{q^2+x^2}-\frac{5}{168}q^2\sqrt{q^2+x^2}-\frac{q^2\sqrt{q^2+x^2}}{10x^2}+\frac{q^4\sqrt{q^2+x^2}}{105x^2}-\frac{5}{168}x^2\sqrt{q^2+x^2}-\frac{x^2\sqrt{q^2+x^2}}{10q^2}+\frac{x^4\sqrt{q^2+x^2}}{105q^2}$$
$$-\frac{\mathbf{P}^2\log(q)}{4x}+\frac{P^4\log(q)}{40x}-\frac{x^2\log(x^2)}{8q}+\frac{x^4\log(x^2)}{80q}+\frac{x^2\log(q)+\sqrt{q^2+x^2}}{4P}+\frac{x^4\log(q)+\sqrt{q^2+x^2}}{40q}+\frac{q^2\log(x)+\sqrt{q^2+x^2}}{4x}-\frac{q^4\log(x)+\sqrt{q^2+x^2}}{40x}$$

$$\frac{\partial[G^2(x,\mathbf{q})]}{2\partial q}=\frac{q^4}{4x^2}-\frac{q^6}{30x^2}+\frac{3}{8}q\sqrt{q^2+x^2}-\frac{1}{15}q^3\sqrt{q^2+x^2}-\frac{q^3\sqrt{q^2+x^2}}{4x^2}+\frac{q^5\sqrt{q^2+x^2}}{30x^2}-\frac{3}{80}qx^2\sqrt{q^2+x^2}-\frac{q^3\log(q)}{2x}+\frac{3q^5\log(q)}{40x}$$
$$-\frac{1}{16}x^2\log(x^2)+\frac{1}{160}x^4\log(x^2)+\frac{1}{8}x^2\log(q+\sqrt{q^2+x^2})-\frac{1}{80}x^4\log(q+\sqrt{q^2+x^2})+\frac{q^3\log(x+\sqrt{q^2+x^2})}{2x}-\frac{3q^5\log(x+\sqrt{q^2+x^2})}{40x}$$

$$\frac{\partial[G^2(x,\mathbf{q})]}{2\partial q}=-\frac{q^4\sqrt{q^2}}{5x^2}+\frac{(q^2)^{\frac{3}{2}}}{x^2}+\frac{\sqrt{q^2+x^2}}{2}-\frac{9q^2\sqrt{q^2+x^2}}{40}-\frac{q^2\sqrt{q^2+x^2}}{x^2}+\frac{q^4\sqrt{q^2+x^2}}{5x^2}-\frac{x^2\sqrt{q^2+x^2}}{20}$$
$$-\frac{3q^2\log(q^2)}{4x}+\frac{3q^4\log(q^2)}{16x}+\frac{3q^2\log(x+\sqrt{q^2+x^2})}{2x}-\frac{3q^4\log(x+\sqrt{q^2+x^2})}{8x}\quad\text{and}\quad\lim_{q\to 0}\frac{\partial[G^2(x,q)]}{2\partial q}=\frac{x}{2}-\frac{x^3}{20}$$

statistical physics which is applied to get information about the microstate from observations of the macrostate.

The first example is the particle size distribution in soils, sediments, or rocks. The grains are not individually measured; instead, a sample is sieved and the finer fractions are determined by indirect methods such as sedimentation. The result is a histogram or an estimated distribution function for each sample. The expected variance is dependent on the sample support. Now, consider samples taken at several supports (holding the shape constant). With a discrete sequence of supports, a sample variance plot can be constructed. This can be used for computing a point variogram with the theory developed before. This same method may be applied to other type of attributes such as pore size distribution in soils. Again variance within a sample depends on sample support.

Another example is from remote sensing. Some authors analyzing fractal dimensions have claimed that multiresolution is required for further research in scale issues (e.g., Quattrochi and Goodchild, 1996). The theory developed here provides a practical justification for multiple resolution. For example, the finest resolution of Landsat images is 30×30 m pixels. Such a resolution comes from the sampling of the reflectance along the scan line called the analog display (Sabins, 1986). In this case, spatial variances could be measured from the analog display signal within several sizes of windows (pixels). Then, a multiresolution imager would provide a set of images and *within* pixels spatial variances for the same episode at increasing resolutions. Those spatial variances can be used to construct a sample variance vs resolution plot, which allows computation of point support variogram.

CONCLUSIONS

The method described in this paper is an alternative to the classic variogram estimator allowing the recovery of point support variogram in cases where point data can not be measured but their spatial variances can be known. Moreover, this method of derivatives of total variance may be the only available tool that recovers the point variogram from variances measured within windows at large support. The meaning of the derivatives of spatial variances was found to be the rate of change of the total variance due to growth of a region. From this it follows that derivatives of variances provide the variogram as the variance of the attribute between two regions of topological dimension zero. The results found also provide a link between the integral of the variogram to spatial variances and to the variogram.

The numerical example shows the approach works as expected. Average variances taken within a growing discrete sequence allow the reconstruction of the variogram. The major complication in practice is to obtain reliable experimental variances or sample dispersion variances. A single coarse resolution variance cannot allow to recover the point variogram and information is lost by averaging.

However, a growing sequence of spatial variances within windows allows to compute the "point" support variogram. Analytical and numerical computations are complicated when the variances come from volumes or surfaces. Therefore, the simplest shape of window is a straight line. Several lines rotated would allow identification of anisotropy in the variance and therefore the directional variograms. The assumption of variances that can be experimentally measured might not be fully adequate in many cases. However, the possibility of measuring sample average variances within windows might be possible with further technological development.

REFERENCES

Clark, I., 1976, Some auxiliary functions for the spherical model of geostatistics: Computers and Geosciences, v. 1, p. 255–263.

Delay, F., and de Marsily, G., 1994, The integral of the semivariogram: A powerful method for adjusting the semivariogram in geostatistics: Math. Geology, v. 26, no. 3, p. 301–321.

Deutsch, C. V., and Journel, A. G., 1992, GSLIB Geostatistical software library and user's guide: Oxford University Press, New York, 340 p.

Journel, A. G., and Huijbregts, Ch. J., 1978, Mining geostatistics: Academic Press, Inc., London, 600 p.

Matheron, G., 1971, Random functions and their application in geology, *in* Merriam, D. F., ed., Geostatistics, a colloquium: Plenum, New York, p. 79–88.

Myers, D. E., Begovich, C. L., Butz, T. R., and Kane, V. E., 1982, Variogram models for regional groundwater geochemical data: Math. Geology, v. 14, no. 6, p. 629–644.

Myers, D. E., 1994, Comments on "Cumulative semivariogram models of regionalized variables" and "Standard cumulative semivariograms of stationary stochastic processes and regional correlation," Letter to the editor: Math. Geology, v. 26, no. 3, p. 415–416.

Quattrochi, D. A., and Goodchild, M. F., 1997, Scale in remote sensing and GIS: Lewis Publishers, New York, 406 p.

Rendu, J. M., 1978, An introduction to geostatistical methods of mineral evaluation: South African Institute of Mining and Metallurgy. Johannesgurg, 84 p.

Sabins, F. F., 1986, Remote sensing, principles and interpretation: W. H. Freeman and Company, New York, 449 p.

Sen, Z., 1989, Cumulative semivariogram models of regionalized variables: Math. Geology, v. 21, no. 8, p. 891–903.

Vargas-Guzmán, J. A., Warrick, A. W., and Myers, D. E., 1999, Multivariate correlation in the framework of support and spatial scales of variability: Math. Geology, v. 31, no. 1, p. 85–103.

Warrick, A. W., and Myers, D. E., 1987, Optimization of sampling locations for variogram calculations: Water Resources Research, v. 23, no. 3, p. 496–500.

Webster, R., and Burgess, T. M., 1984, Sampling and bulking strategies for estimating soil properties in small regions: Journal of Soil Science, v. 35, p. 127–140.